

CrystEngComm

Accepted Manuscript



This is an *Accepted Manuscript*, which has been through the Royal Society of Chemistry peer review process and has been accepted for publication.

Accepted Manuscripts are published online shortly after acceptance, before technical editing, formatting and proof reading. Using this free service, authors can make their results available to the community, in citable form, before we publish the edited article. We will replace this *Accepted Manuscript* with the edited and formatted *Advance Article* as soon as it is available.

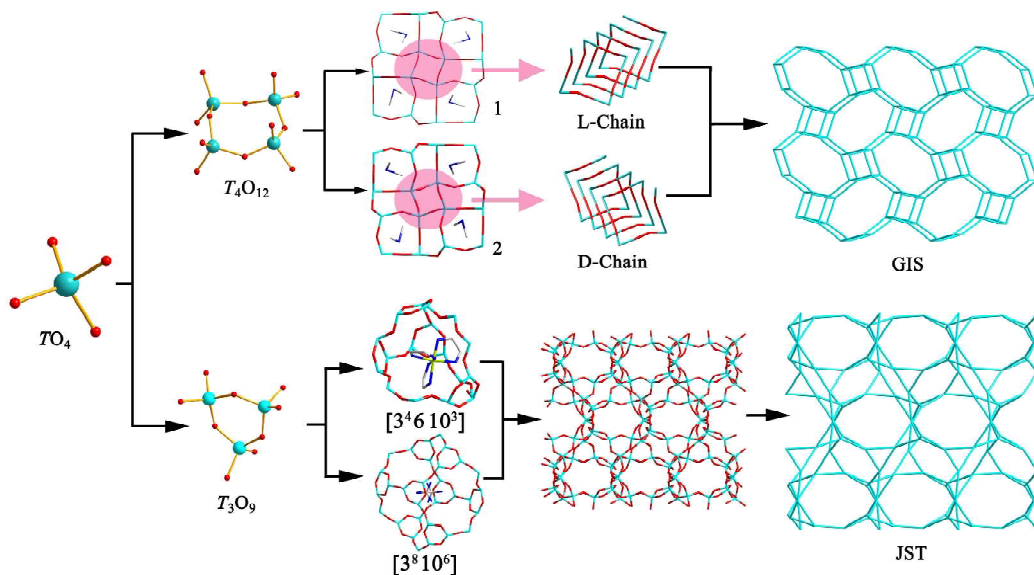
You can find more information about *Accepted Manuscripts* in the [Information for Authors](#).

Please note that technical editing may introduce minor changes to the text and/or graphics, which may alter content. The journal's standard [Terms & Conditions](#) and the [Ethical guidelines](#) still apply. In no event shall the Royal Society of Chemistry be held responsible for any errors or omissions in this *Accepted Manuscript* or any consequences arising from the use of any information it contains.

Table of Contents

Synthesis and Structural Characterization of Three 3-D Aluminogermanates with Different Topologies

Jiahong Wang,^a Yu Zhang,^{*,b} Zaichao Zhang^b and Yan Xu^{*,a}



Compounds **1** and **2** are enantiomers with a GIS topology, while **3** has a JST topology. These three zeolites are all constructed by small rings formed by TO_4 ($T = \text{Ge or Al}$) tetrahedra with different inorganic topological frameworks.

Synthesis and Structural Characterization of Three 3-D Aluminogermanates with Different Topologies

Jiahong Wang,^a Yu Zhang,^{*,b} Zaichao Zhang^b and Yan Xu^{*,a}

^a College of Chemistry and Chemical Engineering, State Key Laboratory of Materials-Oriented Chemical Engineering, Nanjing University of Technology, Nanjing 210009, P. R. China

^b Huai'an Key Laboratory for Photoelectric Conversion and Energy Storage Materials, Jiangsu Key Laboratory for the Chemistry of Low-dimensional Materials, School of Chemistry and Chemical Engineering, Huaiyin Normal University, 111 West Changjiang Road, Huai'an 223300, Jiangsu, People's Republic of China

Three 3-D aluminogermanates L-[C₂NH₈][AlGe₃O₈] **1**, D-[C₂NH₈][AlGe₃O₈] **2** and [Ni(en)₃][Al₃Ge₃O₁₂(H₂en)_{0.5}] **3**, (en = 1, 2-ethanediamine) have been successfully synthesized through hydrothermal synthesis method (**1** and **2** were obtained as a mixture in one autoclave). Crystal structural analysis reveals that three compounds **1**, **2** and **3** are built up of GeO₄ (AlO₄) tetrahedra. Compounds **1** and **2** with typical GIS topology are composed of 4-rings, while **3** is constructed exclusively by 3-rings with JST topology. Compounds **1** and **2** are the enantiomers, and crystallize in chiral space group *P*4₃2₁2 and *P*4₁2₁2, respectively. In compound **3**, rigid chiral transition-metal complex cations, [Ni(en)₃]²⁺, and protonated ethylenediamine cations work as structure directing agents (SDAs) together and induce two different kinds of cages ([3⁸.10⁶] and [3⁴.6.10³]), which further construct the final structure.

Introduction

New open-framework materials have been widely considered and applied in the area of materials chemistry because of their great impact in catalysis, separation, and ion exchange.¹⁻² Among these materials, zeolites with their pure inorganic pores and great thermal stability apparently work better in industry than others in the past decades.³ In this field, chiral zeolite is particularly important due to its special activity in asymmetric catalysis, however, only a few zeolite frameworks with chirality have been reported yet.⁴⁻⁵ As is known to all, zeolites are constructed with TO_4 tetrahedrons through their long-range ordered arrangement. Traditionally, chemists use Si, P, Al etc. as T atoms to build T–O tetrahedra. With the development of the technology in chemical synthesis, boron, gallium and transition metals have been also chosen to use in the synthesis of zeolites. Since the report of the first three open-framework germanates in the early 1990s by Xu,⁶⁻⁷ a number of germanates with various frameworks and pore shapes have been obtained.⁸⁻¹²

Germanium often adopts flexible coordination mode, such as GeO_4 tetrahedron, GeO_5 square pyramid, trigonal bipyramid and GeO_6 octahedron. What's more, Ge–O distance is longer than Si–O distance, Ge–O–Ge angle is smaller than Si–O–Si angle, which makes it easier to build small rings (3-rings and 4-rings) and further construct different kinds of structures with large pores and new topologies (JBW, NAT, CAN, ABW, MON, ANA, RHO, GIS, FAU and JST).¹³⁻²⁴ However, most of these germanates show poor performance in thermal stability.

Nowadays, traditional zeolites such as silicates and aluminum phosphates still work well in the industry because of their great thermal stability. Si and Al atoms with small atomic radius can form short bond distances which have better rigidity than germanium. If Al can be introduced into germanates, the rigidity of skeleton in zeolites may be more enhanced. On the basis of above mentioned considerations, we tried to introduce Al element into germanates and adjust the proportion of germanium and aluminum in order to get new open framework materials with better thermal stability.

In this paper, we report the synthesis and structural characterizations of three 3-D framework aluminogermanates by using different SDAs. Structural analysis indicates

that chiral zeolites **1** and **2** are enantiomers with typical GIS topologies and are both constructed from $[4^6.8^3]$ cages and helical $[-T-O-]_n$ chains, while zeolite **3** $[\text{Ni}(\text{en})_3][\text{Al}_3\text{Ge}_3\text{O}_{12}(\text{H}_2\text{en})_{0.5}]$ is directed by two kinds of SDAs. In **3**, ethylenediamine (en) induces $[3^4.6.10^3]$ cage while the rigid chiral transition-metal complex cation $[\text{Ni}(\text{en})_3]^{2+}$ induces $[3^8.10^6]$ cage.

Experimental

Materials and measurements

All chemicals purchased were of reagent grade and used without further purification. IR spectrum was recorded on a Nicolet Impact 410 FTIR spectrometer using KBr pellets in $4000\text{-}400\text{ cm}^{-1}$ region. For **1** and **2**, thermogravimetric analyses were carried out in N_2 atmosphere on a diamond thermogravimetric analyzer from 50 to 600 °C with a heating rate of 10 °C/min. For **3**, thermogravimetric analyses were carried out in N_2 atmosphere on a diamond thermogravimetric analyzer from 50 to 800 °C with a heating rate of 10 °C/min. Single-crystal X-ray diffraction data for these compounds were collected on a Bruker Smart Apex II CCD diffractometer using graphite-monochromated Mo $K\alpha$ radiation ($\lambda = 0.71073\text{ \AA}$) at the temperature of 293K. X-ray photoelectron spectroscopy (XPS) uses S-Probe ESCA model 2803 (Fision Instrument, 10 kV, 20 mA) with Al $K\alpha$ as X-rays source.

Synthesis of mixed L- $[\text{C}_2\text{NH}_8][\text{AlGe}_3\text{O}_8]$ and D- $[\text{C}_2\text{NH}_8][\text{AlGe}_3\text{O}_8]$ (**1** and **2**)

Compounds **1** and **2** were obtained as a mixture in one autoclave. Due to the same crystal shape of these two compounds, it is very difficult to separate them. In the process of characterization, we used the mixture of **1** and **2**. A mixture of GeO_2 (0.1002 g, 0.9543 mmol), Al_2O_3 (0.1009 g, 0.9892 mmol), N, N-dimethylformamide (6.0127 g, 82.37 mmol), deionized water (0.5002 g, 27.79 mmol) and N-methylpiperazine (1.5090 g, 16.05 mmol) with a molar ratio of 1 : 1 : 86 : 29 : 17 was stirred in open air for 6 hours, and 40% hydrofluoric (0.3 ml, 0.6012 mmol) was added to the mixture. Then, the suspension was stirred for an additional 20 min and transferred to a 30 mL Teflon-lined autoclave. After being heated at 170 °C for 7 days,

octahedron crystals of mixture of **1** and **2** were obtained in one autoclave. None further isolation has been done due to the same crystal shape of these two compounds (Fig.S1a). Yield: 0.0662 g, 47.4% (based on Ge^{IV}). Anal (%) Calcd for C₂H₈NAIGe₃O₈: C 5.73, H 1.91, N 3.34. Found: C 5.81, H 1.99, N 3.43. IR of mixed compounds **1** and **2** (cm⁻¹): 3445 s, 3171 m, 2971 w, 2922 w, 1630 s, 1467 s, 1389 s, 981 m, 893 m, 596 w, 465 w.

Synthesis of [Ni(en)₃][Al₃Ge₃O₁₂(H₂en)_{0.5}] (**3**)

A mixture of GeO₂ (0.1020 g, 0.9808 mmol), Al₂O₃ (0.1023 g, 1.003 mmol), deionized water (0.4235 g, 23.53 mmol), glycol (1.8155 g, 29.28 mmol), 1,2-ethanediamine (0.8622 g, 14.37 mmol) and Tetraethylenepentamine (0.6848 g, 3.623 mmol) with a molar ratio of 1 : 1 : 24 : 29 : 14 was stirred in open air for 3 hours, and Ni(Ac)₂·4H₂O (0.1320 g, 0.5301 mmol) and 40% hydrofluoric (0.04 ml, 0.0802 mmol) were added into the mixture. Then the suspension was stirred for another three hours. Finally, the suspension was transferred into a 30 ml Teflon-lined stainless steel autoclave. After being heated at 170 °C for 7 days, peak octahedron crystals of **3** were obtained (Fig.S1b). Yield: 0.1041 g, 39.5% (based on Ge^{IV}). Since excessive amounts of en were used, and the suspension (reactants) was stirred in open air for 3 hours, the [Ni(en)₃]⁺² species was formed from the Ni(ac)₂·4H₂O and excess en. Then the [Ni(en)₃]⁺² and protonated ethylenediamine cations work as SDAs together. Anal (%) Calcd for C₇N₇H₂₉NiAl₃Ge₃O₁₂: C 11.04, N 12.88, H 3.81. Found: C 12.14, N 14.17, H 4.17. IR of compound **3** (cm⁻¹): 3442 w, 3288 s, 3193 m, 2958 s, 2896 w, 1596 s, 1037 s, 852 s, 766 m, 604 s, 445 w.

XPS results

The XPS analysis was based on the areas of the peaks Al 2p and Ge 3d using the following equation

$$C_i = (I_i/S_i) [\sum(I_i/S_i)]^{-1}$$

with $i = 1, n$, where C_i is the atomic percentage of element i , I_i is the intensity of the photoelectron signal obtained by the peak area after subtraction of a linear

background and S_i is the atomic sensitivity calculated using the cross-section of Scofield²⁵, corrected for the angular asymmetry function $L(\gamma)$, with $\gamma = 49.1^\circ$ for the instrument used. For the determination of this angular function $L(\gamma)$, the asymmetry parameter from Reilman *et al.*²⁶ has been used.

XPS spectra of aluminium (Al 2p) and germanium (Ge 3d) of the mixed compounds **1** and **2** are shown in Fig.1a and Fig.1b, while Fig.1c and Fig.1d present XPS spectra of **3**. After fitting and calculation, we found that the atomic percentages of Al and Ge are 4.86% and 13.55% for the mixed compounds **1** and **2**, which indicate the atomic ratio of Al/Ge is 1/3. In compound **3**, the atomic percentage of Al is 17.69%, while the atomic percentage of Ge is 16.04%, which indicate the atomic ratio of Al/Ge is 1/1.

Structure determination

Data processing was accomplished with the SAINT processing program. The structures of all compounds were solved by direct methods and refined on F^2 by full matrix least-squares techniques with SHELXTL-97 software package²⁷. All non-hydrogen atoms were refined anisotropically. In compounds **1** and **2**, the DMA cation is found to be disordered in the structure and has two different orientations. In compound **3**, both ethylenediamine and $[\text{Ni}(\text{en})_3]^{2+}$ cations are found to be disordered in the structure. Since free ethylenediamine cation is disordered and has three different orientations, hydrogen atoms in ethylenediamine cation are not added. The crystallographic data and details of data collection and structure refinement of these compounds are given in Table 1 and selected bond distances and angles are listed in supporting information.

Results and discussion

Powder XRD patterns (Cu $K\alpha$ radiation)

Fig.2a presents the powder X-ray diffraction patterns for the mixture of compounds **1** and **2**, while Fig.2d shows the powder X-ray diffraction patterns for **3**. Diffraction peaks of both the simulated and experimental patterns are well-matched in relevant

positions.

Structure description

Single-crystal X-ray diffraction analysis reveals that **1** and **2** are enantiomers. Zeolite **1** crystallizes in chiral space group of $P4_32_12$. Three distinct T sites (T1, T2 and T3) are tetrahedrally coordinated by four oxygen atoms (Fig.3). Each T site in the framework of **1** is occupied by AlO_4 or GeO_4 tetrahedra with the Al/Ge ratio of 0.25:0.75, which is in agreement with the XPS results. As show in Fig.4a, adjacent four TO_4 tetrahedrons are connected to each other by sharing the vertices to generate a four-membered ring T_4O_{12} , which is worked as a secondary building unit and further constructs the GIS topological inorganic framework. Along a or b axis, neighbouring four-membered rings are connected to each other in an up and down arrangement by sharing the vertices to form a band structure, which is considered as a typical band structure in zeolites (Fig.4b). Cross-connected bands form two-dimensional (2D) structure in $0\ 0\ 1$ direction, and then further linked by sharing vertices of TO_4 tetrahedrons to form a 3D framework. Eight-membered ring channels can be found along a and b axis. It is easy to see that, in ac plane, every four-membered ring is connected to the adjacent four four-membered rings directly by sharing vertices and surrounded by four eight-membered ring channels, as shown in Fig.4c. The channel opening size of eight-membered ring is about $6.7 \times 9.1 \text{ \AA}^2$. Four eight-membered rings and six four-membered rings are connected to each other by sharing the edges to form a $[4^6.8^4]$ cage (Fig.5a). The protonated dimethylamine cation is located in the center of cage and directed this $Ge(Al)-O [4^6.8^4]$ cage through hydrogen bonding interactions, and fit the symmetry of 4_32_12 by disorder (Fig.5b). The distance of hydrogen bond is in the range of 2.89(2)-3.40(2) for $N-H\cdots O$ and 3.28(2)-3.47(2) \AA for $C-H\cdots O$, respectively (Fig.S2). Interestingly, every four 4-membered ring channels along c axis, is enclosed by a left-handed $[-T-O-]_n$ chain, as show in Fig.6a. The Flack parameter for **1** is of 0.03(5), which indicates that the absolute configuration of **1** is correct. As an enantiomer of **1**, the inorganic framework of zeolite **2** keeps the same topological structure. Correspondingly, **2** crystallizes in another chiral space group

$P4_12_12$. We can find a right-handed $[-T-O-]_n$ chains in **2** (Fig.6b). The Flack parameter of **2** is 0.00(5). We have tried to solve **2** in the space group $P4_32_12$ and **1** in the space group $P4_12_12$, the flack parameters are 0.97(6) and 0.91(6) respectively, which indicates that the absolute configuration of **1** in $P4_12_12$ and **2** in $P4_32_12$ are both wrong. The T–O distances in **1** and **2** are in the range of 1.707(10)–1.782(9) Å, and all T–O–T angles are in the range of 101.5(7)–117.1(6)°, which are reasonable for aluminogermanates²⁸. To the best of our knowledge, chiral zeolites are very rare, while chiral zeolitic aluminogermanate has not been reported until now. Since no clear L or D signals were observed in the solid CD spectrum for the mixture of **1** and **2** (Fig.S3), the ratio of compound **1** : **2** in the mixture should be about 50% : 50%. While the inorganic framework of **1** and **2** will be collapsed after removing organic amine.

Compound **3** crystallizes in the cubic space group $Pa\bar{3}$ with $a = 16.4699(7)$ Å. The building units and inorganic framework compound **3** are similar to the GaGeO-CJ63²⁹ and $[M(II)(en)_3][M(III)_2Ge_4O_{12}]$ ($M(II) = Ni, Co$; $M(III) = Al$; $en = ethylenediamine$)³⁰. The structure of zeolite **3** contains two crystallographically distinct T sites (T = Al, Ge), both T sites are occupied by Al and Ge atoms that are tetrahedrally coordinated by four oxygen atoms with the ratio of 1 : 1 (Al : Ge), which is corresponding to the XPS results. The T–O distances are in the range of 1.739(3)–1.757(3) Å, and all T–O–T angles are in the range of 127.1(2)–131.2(2)°, which are comparable with reported aluminogermanates with 3-rings²⁹. There are two kinds of 3-rings: one of which has C1 symmetry and the other has C3 symmetry. 3-rings with C1 symmetry connect to 3-rings with C3 symmetry to form a spiro-5 secondary building unit, and the spiro-5 units further construct the whole framework³¹. The inorganic framework of **3** has 3D interconnecting 10-ring channels. In the framework of **3**, there are two types of cages including $[3^8.10^6]$ (Fig.7a) and $[3^4.6.10^3]$ cage (Fig.7b). Each $[3^4.6.10^3]$ cage holds one $[Ni(en)_3]^{2+}$ cation, while one protonated ethanediamine cation is located in the $[3^8.10^6]$ cage. $[Ni(en)_3]^{2+}$ cation and protonated ethanediamine not only work as SDAs, but also compensate negative charges. Compared with $[M(II)(en)_3][M(III)_2Ge_4O_{12}]$ ($M(II) = Ni, Co$; $M(III) = Al$; $en = ethylenediamine$),

compound **3** has a higher Al/Ge ratio, nevertheless these zeolites nearly have the same framework structure, which may lead by the protonated ethanediamine (Fig.7c). It proves that the cations of SDAs with higher positive charge may lead to higher Al/Ge ratio. Organic molecules usually adopt the symmetry of inorganic framework by changing the orientation or disorder, which is often observed in the reported organic-directed germanates³². In $[3^8.10^6]$ cage, the protonated ethanediamine cation is situated at a particular position. The inversion center of C(3) and C(3A) locate on triple anti-axis, which is also one of the most important symmetries for the inorganic framework. As show in fig. 7c, the protonated ethanediamine cation adopts the essential symmetry of inorganic framework (triple axis) by disorder, the occupied factor N3 is 1/3. The structure of the ethanediamine cations is important for the formation of the final structure from symmetry considerations. The organic SDAs, $[\text{Ni}(\text{en})_3]^{2+}$ and H_2en cations, are involved weak hydrogen bonding interactions with O atoms of inorganic framework of **3**, as show in Fig.S4a and Fig.S4b. Unfortunately, although the zeolite **3** has a higher Al/Ge ratio, the inorganic framework of **3** is not stable after removing organic SDAs. Fig.S9 shows the Powder XRD patterns of compound **3** which has been heated at 400 °C for about 5 hours.

TG Analysis

TG Analysis of the mixed compounds **1** and **2**

As shown in Fig.S5, the weight loss of 11.03% in the range of 50-600 °C corresponds to the removal of the dimethylamine cations (calc. 10.98%). In order to observe the thermal stability of the skeleton, the sample of thermal gravimetric analysis was used for the powder X-ray diffraction test. The final test results showed that the skeleton has collapsed; the skeleton can not be maintained.

TG Analysis of compound **3**

Thermal analysis shows that the total weight loss is 27.67% (calc. 28.79) as shown in Fig.S6, the weight loss in the range of 50-800 °C corresponds to the removal of the protonated ethylenediamine cations (calc. 5.13%) and en from $[\text{Ni}(\text{en})_3]^{2+}$ cations (calc. 23.66%).

IR Spectra

IR Spectra of the mixed compounds **1** and **2**

The IR spectrum of the mixture **1** and **2** (Fig.S7) exhibits two peaks at 981 and 893 cm^{-1} associated with ν^{as} (Ge–O–Ge) and two peaks at 596, 510 cm^{-1} are due to ν^{s} (Ge–O–Ge). The absorption peak at 465 cm^{-1} peak is identified as a Ge–O bending vibration. It also possesses bands in 3445–3171 cm^{-1} region which can be attributed to ν (N–H) and bands between 1400 to 1630 cm^{-1} are assigned to the C–N stretching vibrations of dimethylamine. C–H stretching vibration and bending vibration absorption peaks located at 2971, 2922 cm^{-1} and 1467, 1389 cm^{-1} respectively.

IR Spectra of compound **3**

The IR spectrum of compound **3** (Fig.S8) exhibits two peaks at 852 and 766 cm^{-1} associated with ν^{as} (Ge–O–Ge) and two peaks at 596, 510 cm^{-1} are due to ν^{s} (Ge–O–Ge). The peak at 445 cm^{-1} peak is identified as a Ge–O bending vibration. It also possesses bands in 3193–3442 cm^{-1} region which are attributed to ν (N–H) and bands between 1400 to 1600 cm^{-1} are assigned to the C–N stretching vibrations of ethylenediamine.

Conclusion

Three aluminogermanates have been successfully obtained. Compounds **1** and **2** are enantiomers with a GIS topology by using dimethylamine cations as SDA, while $[\text{Ni}(\text{en})_3]^{2+}$ and en cations work as SDAs together to induce two different kinds of cages ($[3^8.10^6]$ and $[3^4.6.10^3]$) in **3**. These three zeolites are all constructed by small rings formed by TO_4 ($T = \text{Ge}$ or Al) tetrahedra with different inorganic topological frameworks. Unfortunately, the inorganic frameworks of three aluminogermanates are not stable after removing organic SDAs. The successful synthesis of these three compounds demonstrates new zeolitic aluminogermanates with different topology or compositions can be synthesized by using different SDAs.

Supplementary data

CCDC 977878, 977877 and 977879 contain the supplementary crystallographic data for compound **1**, **2** and **3**. These data can be obtained free of charge via <http://www.ccdc.com.ac.uk/conts/retrieving.html>, or from Cambridge Crystallographic Data Centre, 12 Union Road, Cambridge CB2 1E2, UK; fax: (+44) 1223-336-033; or e-mail: deposit@ccdc.cam.ac.uk.

Associated contentment

This work is financially supported by Natural Science Foundation of Jiangsu Province (Grant BK2012823 and BK20131212), the Project of Priority Academic Program Development of Jiangsu Higher Education Institutions (PAPD), National Science Foundation of Educational Commission of Jiangsu Province of China (Nos.12KJA150004).

Author Information

Corresponding Author

*E-mail: yanxu@njut.edu.cn (Y. Xu). Tel: 86-25-83587857. Fax: 86-25-83211563.

yuzhang@hytc.edu.cn (Y. Zhang)

Notes and references

- 1 A. K. Cheetham, G. Ferey and T. Loiseau, *Angew. Chem., Int. Ed.*, 1999, **38**, 3268.
- 2 M. E. Davis, *Nature*, 2002, **417**, 813.
- 3 J. H. Yu, R. R. Xu, *Accounts Chem. Res.*, 2010, **43**, 1195.
- 4 C. Baerlocher, L. B. McCusker, D. H. Olson, *Atlas of Zeolite Framework Types*, 6th rev. ed., Elsevier, Amsterdam, 2007.
- 5 J. L. Sun, A. Corma, X. D. Zou, *Nature*, 2009, **458**, 1154.
- 6 J. Cheng, R. R. Xu, *J. Chem. Soc. Chem. Comm.*, 1991, **7**, 483.
- 7 R. Jones, J. Chen, J. M. Thomas, A. George, M. B. Hursthouse, R. Xu, *Chem Mater*, 1992, **4**, 808.
- 8 J. Plévert, T. M. Gentz, A. Laine, H. L. Li, V. G. Young, O. M. Yaghi, M. O'Keeffe, *J. Am. Chem. Soc.*, 2001, **123**, 12706.
- 9 Y. Zhou, H. Zhu, Z. Chen, M. Chen, Y. Xu, D. Y. Zhao, *Angew. Chem. Int. Ed.*, 2001, **40**, 2166.
- 10 K. E. Christensen, C. Bonneau, M. Gustafsson, L. Shi, X. D. Zou, *J. Am. Chem. Soc.*, 2008, **130**, 3758.
- 11 Q. H. Pan, J. Li, K. E. Christensen, C. Bonneau, X. D. Zou, J. H. Yu, R. R. Xu, *Angew Chem. Int.*

- Ed.*, 2008, **47**, 7868.
- 12 X. Y. Ren, J. H. Yu, R. R. Xu, *J. Am. Chem. Soc.*, 2009, **131**, 14128.
- 13 C. T. Kresge, M. E. Leonowicz, W. J. Roth, J. C. Vartuli, J. S. Beck, *Nature*, 1992, **359**, 710.
- 14 D. Y. Zhao, *Science*, 1998, **279**, 548.
- 15 O. Terasaki, *Mesoporous and Related Nano-structured Materials* (Elsevier, New York, 2004).
- 16 X. D. Zou, T. Conradsson, M. Klingstedt, M. S. Dadachov, M. O'Keeffe, *Nature*, 2005, **437**, 716.
- 17 A. M. Healey, P. F. Henry, G. M. Johnson, M. T. Weller, M. Webster, A. J. Genge, *Microporous Mesoporous Mater.*, 2000, **37**, 165.
- 18 A. Tripathi, M. Johnson, S. J. Kim, *Mater. Chem.* 2000, **10**, 451.
- 19 Y. Lee, J. B. Parise, A. Tripathi, S. J. Kim, T. Vogt, *Microporous Mesoporous Mater.* 2000, **39**, 445.
- 20 A. Tripathi, S. J. Kim, G. M. Johnson, J. B. Parise, *Microporous Mesoporous Mater.* 2000, **34**, 273.
- 21 A. Tripathi, J. B. Parise, *Microporous Mesoporous Mater.* 2002, **52**, 65.
- 22 G. M. Johnson, A. Tripathi, J. B. Parise, *Microporous Mesoporous Mater.* 1999, **28**, 139.
- 23 G. M. Johnson, A. Tripathi, J. B. Parise, *Chem. Mater.* 1999, **11**, 10.
- 24 A. J. Celestian, J. B. Parise, C. Goodell, A. Tripathi, J. Hanson, *Chem. Mater.* 2004, **16**, 2244.
- 25 J. H. Scofield, *J. Electron Spectrosc. Relat. Phenom.* 1976, **8**, 129.
- 26 R. F. Reilman, A. Msezane, S. T. Manson, *J. Electron Spectrosc. Relat. Phenom.* 1976, **8**, 389.
- 27 Sheldrick, G. M., *SHELX97, Programs for Crystal Structure Analysis*; University of Göttingen: Göttingen, Germany, 1997 (release 97-2).
- 28 G. M. Johnson, M. T. Weller, *Inorg. Chem.* 1999, **38**, 2442.
- 29 Y. D. Han, J. H. Yu, *Angew. Chem. Int. Ed.* 2011, **50**, 3003.
- 30 Y. Xu, Y. Li, J. H. Yu, *Dalton Trans.* 2012, **41**, 12170.
- 31 J. Su, Y. X. Wang, J. H. Lin, *J. Am. Chem. Soc.*, 2009, **131**, 6080.
- 32 X. C. Sun, Y. Xu, *Z. Anorg. Allg. Chem.* 2009, 2596.

Table 1. Crystal Data and Structure Refinements for 1 and 2

| | L-1 | D-1 | 2 |
|--|--|--|---|
| formula | [C ₂ NH ₈][AlGe ₃ O ₈] | [C ₂ NH ₈][AlGe ₃ O ₈] | [Ni(en) ₃][Al ₃ Ge ₃ O ₁₂ (H ₂ en) _{0.5}] |
| fw | 418.84 | 418.84 | 760.79 |
| <i>T</i> (K) | 293(2) | 296(2) | 293(2) |
| wavelength (Å) | 0.71073 | 0.71073 | 0.71073 |
| cryst syst | Tetragonal | Tetragonal | Cubic |
| space group | <i>P</i> 4 ₃ 2 ₁ 2 | <i>P</i> 4 ₁ 2 ₁ 2 | <i>Pa</i> $\bar{3}$ |
| <i>a</i> (Å) | 10.3404(3) | 10.3388(7) | 16.4699(7) |
| <i>b</i> (Å) | 10.3404(3) | 10.3388(7) | 16.4699(7) |
| <i>c</i> (Å) | 9.4021(7) | 9.4073(12) | 16.4699(7) |
| α (deg) | 90 | 90 | 90 |
| β (deg) | 90 | 90 | 90 |
| γ (deg) | 90 | 90 | 90 |
| <i>V</i> (Å ³) | 1005.31(9) | 1005.55(16) | 4467.6(3) |
| <i>Z</i> | 4 | 4 | 8 |
| <i>D</i> _c (mg/m ³) | 2.768 | 2.767 | 2.262 |
| μ (mm ⁻¹) | 9.023 | 9.021 | 5.018 |
| <i>F</i> (000) | 800 | 800 | 3032 |
| cryst size (mm ³) | 0.13 × 0.13 × 0.12 | 0.13 × 0.13 × 0.12 | 0.12 × 0.12 × 0.12 |
| limiting indices | -12 ≤ <i>h</i> ≤ 12, -12 ≤ <i>k</i> ≤ 12, -11 ≤ <i>l</i> ≤ 11 | -10 ≤ <i>h</i> ≤ 12, -12 ≤ <i>k</i> ≤ 11, -11 ≤ <i>l</i> ≤ 11 | -18 ≤ <i>h</i> ≤ 20, -20 ≤ <i>k</i> ≤ 20, -13 ≤ <i>l</i> ≤ 20 |
| θ range (deg) | 2.79–25.50 | 2.79–25.01 | 2.14–25.94 |
| reflns collected | 7403 | 7149 | 22677 |
| <i>R</i> (int) | 0.0285 | 0.0367 | 0.0717 |
| data / restraints / param | 940 / 7 / 77 | 901 / 24 / 74 | 1466 / 6 / 115 |
| Flack param | 0.03(5) | 0.00(5) | |
| GOF | 1.125 | 1.057 | 1.136 |
| <i>R</i> 1 ^a , <i>wR</i> 2 ^b [<i>I</i> > 2 σ (<i>I</i>)] | 0.0253, 0.0756 | 0.0288, 0.1166 | 0.0389, 0.1193 |
| <i>R</i> 1, <i>wR</i> 2 (all data) | 0.0271, 0.0765 | 0.0306, 0.1179 | 0.0500, 0.1243 |

^a*R*1 = $\Sigma||F_o| - |F_c||/\Sigma|F_o|$. ^b*wR*2 = $\Sigma[w(F_o^2 - F_c^2)^2]/\Sigma[w(F_o^2)^2]^{1/2}$.

Figure Captions

Fig.1 XPS result for the mixture of compounds **1** and **2**. (a) Binding energy for highest peak is 73.400 eV, peak area is 486.149, FWHM is 2.340, GL(%) is 18; (b) Binding energy for highest peak is 31.780 eV, peak area is 2990.246, FWHM is 1.500, GL(%) is 5; (c) Binding energy for highest peak is 72.770 eV, peak area is 685.465, FWHM is 1.510, GL(%) is 5; (d) Binding energy for highest peak is 30.820 eV, peak area is 1227.684, FWHM is 1.430, GL(%) is 5.

Fig.2 Powder XRD patterns of compounds **1-3**. (a) The powder XRD patterns of the mixture of compounds **1** and **2**; (b) The simulated XRD pattern of compound **1**; (c) The simulated XRD pattern of compound **2**; (d) The powder XRD patterns of compound **3**; (e) The simulated XRD pattern of **3**.

Fig.3 The asymmetric unit of compound **1**.

Fig.4 (a) T_4O_{12} ring in compound **1**; (b) The band formed by 4-rings in compound **1**; (c) The layer formed by 4-rings and 8-rings in compound **1**.

Fig.5 (a) A $[4^68^3]$ cage in compound **1**; (b) The protonated dimethylamine in $[4^68^3]$ cage. Symmetry codes: (a) 1-y, 1-x, -0.5-z.

Fig.6 (a) L-[-T-O-] $_n$ chain in compound **1**; (b) D-[-T-O-] $_n$ chain in compound **2**.

Fig.7 (a) A $[3^8.10^6]$ cage in compound **3**; (b) A $[3^4.6.10^3]$ cage in compound **3**, the inversion center of C(3) and C(3A) locate on triple anti-axis, which is also one of the most important symmetries for the inorganic framework; (c) Disordered ethylenediamine. Symmetry codes: (a) z, x, y; (b) y, z, x; (c) 1-x, 1-y, 1-z; (d) 1-z, 1-x, 1-y; (e) 1-y, 1-z, 1-x.

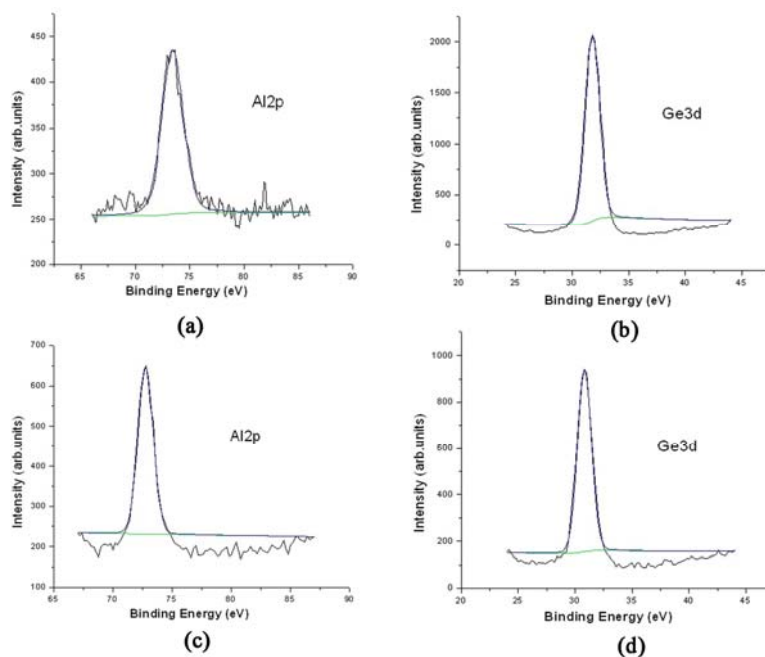


Fig.1 XPS result for the mixture of compounds **1** and **2**. (a) Binding energy for highest peak is 73.400 eV, peak area is 486.149, FWHM is 2.340, GL(%) is 18; (b) Binding energy for highest peak is 31.780 eV, peak area is 2990.246, FWHM is 1.500, GL(%) is 5; (c) Binding energy for highest peak is 72.770 eV, peak area is 685.465, FWHM is 1.510, GL(%) is 5; (d) Binding energy for highest peak is 30.820 eV, peak area is 1227.684, FWHM is 1.430, GL(%) is 5.

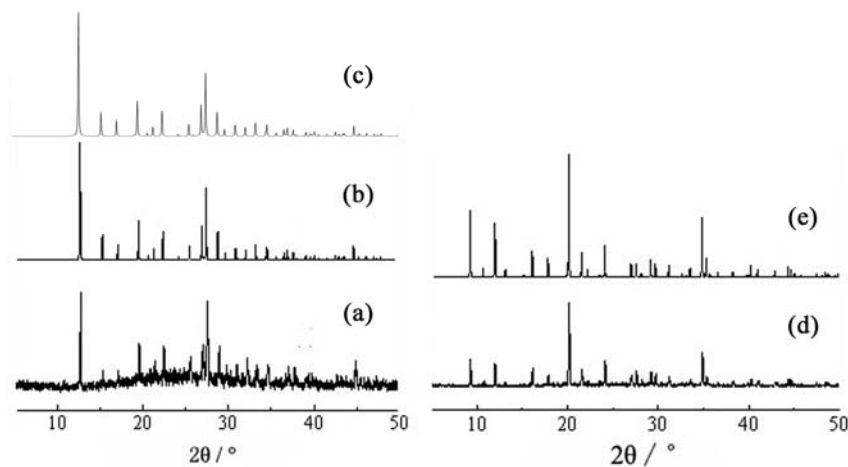


Fig.2 Powder XRD patterns of compounds **1-3**. (a) The powder XRD patterns of the mixture of compounds **1** and **2**; (b) The simulated XRD pattern of compound **1**; (c) The simulated XRD pattern of compound **2**; (d) The powder XRD patterns of compound **3**; (e) The simulated XRD pattern of **3**.

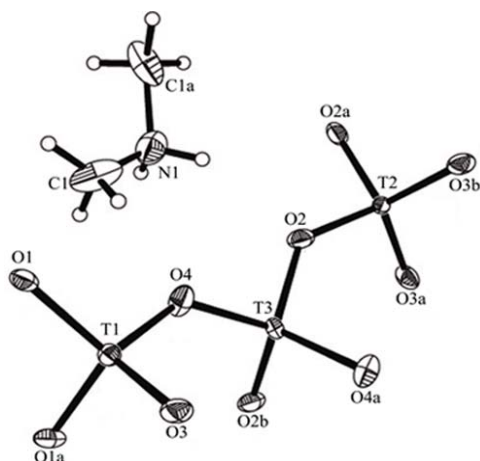


Fig.3 The asymmetric unit of compound **1**. Symmetry codes: (a) $1-y, 1-x, -0.5-z$; (b) $0.5-y, 0.5+x, -0.25+z$.

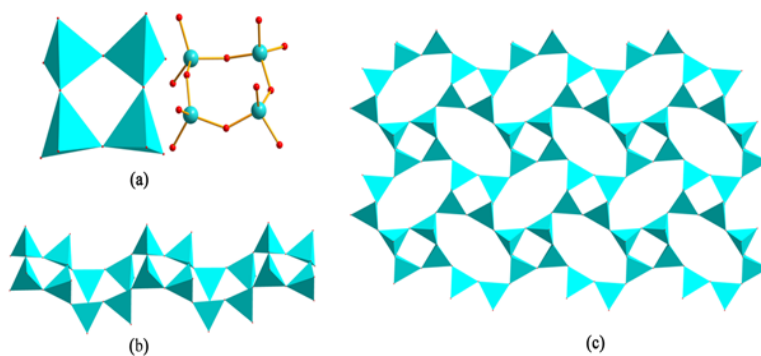


Fig.4 (a) T_4O_{12} ring in compound **1**; (b) The band formed by 4-rings in compound **1**; (c) The layer formed by 4-rings and 8-rings in compound **1**.

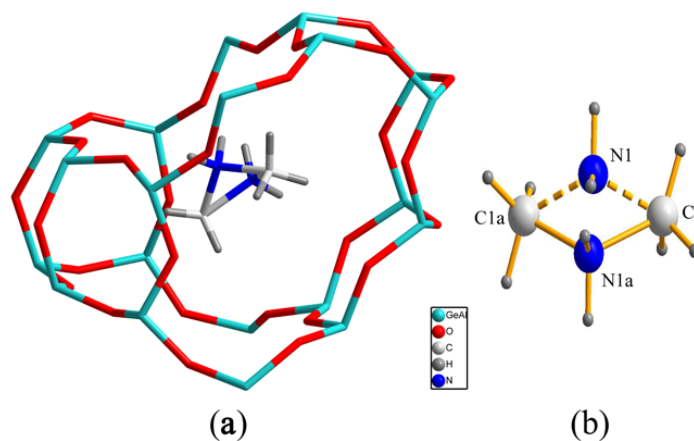


Fig.5 (a) A $[4^6 8^3]$ cage in compound **1**; (b) The protonated dimethylamine in $[4^6 8^3]$ cage. Symmetry codes: (a) $1-y, 1-x, -0.5-z$.

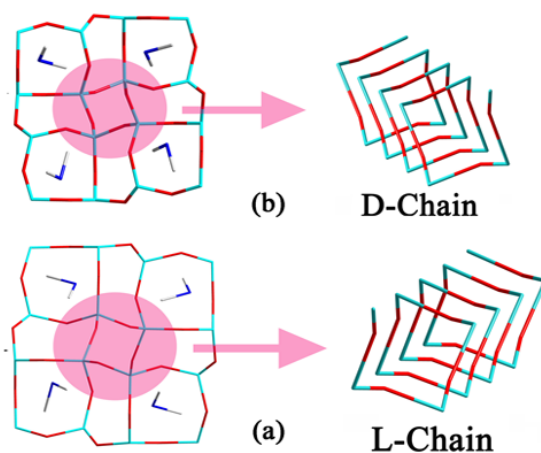


Fig.6 (a) L-[-T-O-] n chain in compound **1**; (b) D-[-T-O-] n chain in compound **2**.

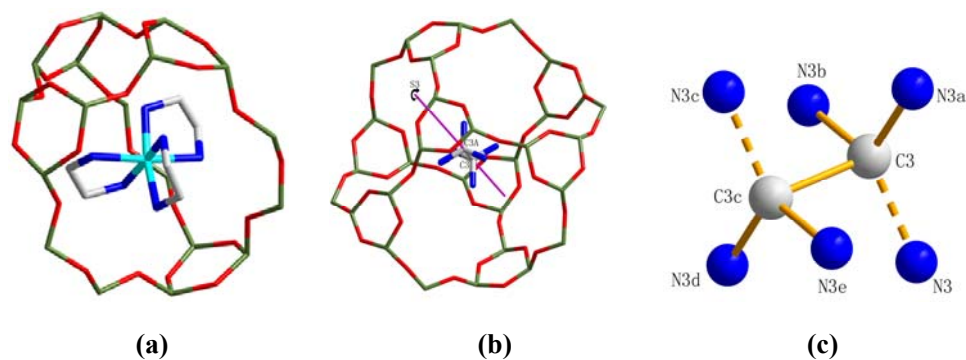


Fig.7 (a) A $[3^8.10^6]$ cage in compound **3**; (b) A $[3^4.6.10^3]$ cage in compound **3**, the inversion center of C(3) and C(3A) locate on triple anti-axis, which is also one of the most important symmetries for the inorganic framework; (c) Disordered ethylenediamine. Symmetry codes: (a) z, x, y ; (b) y, z, x ; (c) $1-x, 1-y, 1-z$; (d) $1-z, 1-x, 1-y$; (e) $1-y, 1-z, 1-x$.